AIP | Journal of Applied Physics

Room temperature multiferroic properties and magnetoelectric coupling in Sm and Ni substituted Bi4− x Sm x Ti3− x Ni x O12±δ (x=0, 0.02, 0.05, 0.07) ceramics

Joginder Paul, Sumit Bhardwaj, K. K. Sharma, R. K. Kotnala, and Ravi Kumar

Citation: Journal of Applied Physics **115**, 204909 (2014); doi: 10.1063/1.4880159
View online: http://dx.doi.org/10.1063/1.4880159
View Table of Contents: http://scitation.aip.org/content/aip/journal/jap/115/20?ver=pdfcov
Published by the AIP Publishing

Room temperature multiferroic properties and magnetoelectric coupling in Sm and Ni substituted $Bi_{4-x}Sm_xTi_{3-x}Ni_xO_{12\pm\delta}$ ($x = 0, 0.02, 0.05, 0.07$) ceramics

Joginder Paul,[1,a)] Sumit Bhardwaj,[1] K. K. Sharma,[2] R. K. Kotnala,[3] and Ravi Kumar[1,4]
[1]*Centre for Materials Science and Engineering, National Institute of Technology, Hamirpur, Himachal Pradesh 177 005, India*
[2]*Department of Physics, National Institute of Technology, Hamirpur, Himachal Pradesh 177 005, India*
[3]*National Physical Laboratory, New Delhi 110 012, India*
[4]*Beant College of Engineering and Technology, Gurdaspur, Punjab 143 521, India*

(Received 7 February 2014; accepted 15 May 2014; published online 28 May 2014)

Lead free multiferroic $Bi_{4-x}Sm_xTi_{3-x}Ni_xO_{12\pm\delta}$ ($x = 0.02$, 0.05, and 0.07) samples have been synthesized by conventional solid state route. X-ray diffraction analysis reveals single phase up to $x = 0.07$, and a secondary phase appears at $x > 0.07$. Raman spectroscopy confirms the local distortions in the crystal. Field emission scanning electron microscopy shows plate like grains. Substitution has increased the orthorhombic distortion, grain size, and hence the ferroelectric transition temperature (T_c). A significant reduction in the values of dielectric constant (ε') and loss tangent ($\tan\delta$) has been observed with the increase of Sm and Ni ions. The increase in dc resistivity at room temperature has been found with substitution. Enhancement in the values of remnant polarization ($2P_r$) and magnetization ($2M_r$) is observed. Magnetoelectric coupling coefficient (α) values of 0.60 mV/cm/Oe are achieved in $Bi_{4-x}Sm_xTi_{3-x}Ni_xO_{12\pm\delta}$ ceramic samples. Hence, we have successfully converted the ferroelectric $Bi_4Ti_3O_{12}$ into a multiferroic, which is a new lead free multiferroic material, can be useful for future electromagnetic devices. © *2014 AIP Publishing LLC*. [http://dx.doi.org/10.1063/1.4880159]

I. INTRODUCTION

In recent years, multiferroic materials have attracted considerable attention due to their potential applications in multifunctional devices, such as data storage devices, multiple state memory elements, transducers, and sensors.[1,2] The simultaneous occurrence of both ferroelectric and ferromagnetic order in a single material is very interesting and fascinating.[3,4] The interaction between the two ferroic orders manifest itself as a magnetoelectric (ME) effect, i.e., electric polarization is induced by changing magnetic field or magnetization is induced by changing electric field.[5,6] However, the materials showing both electric polarization and magnetization are few in number. The co-existence of these ferroic orders at room temperature is of both the technological and fundamental interest. Moreover, the coupling between these two order parameters provides an extra degree of freedom in device designing, which makes it possible to write data bit with an electric field and read it with magnetic field, and vice-versa.[7,8] However, the mechanisms for ferroelectricity and ferromagnetism are mutually exclusive to each other.[9,10] Ferroelectricity requires empty d-orbitals, whereas magnetism needs partially or half filled d-orbitals.[7] Therefore, single phase multiferroic materials are rare and out of those which are known, still have small magneto-electric effect at room temperature and cannot be useful for practical applications. So the search for single phase multiferroic materials having large magnetoelectric effect at or above room temperature still continues.

Many multiferroic compounds such as $YMnO_3$, Cr_2O_3, and $TbMnO_3$ have been studied during the last decade.[11–13] The magnetoelectric effect in these materials at room temperature is small. Among the multiferroic materials, $BiFeO_3$ is the extensively studied compound. It exhibits magnetoelectric effect at room temperature, but high electrical conductivity and phase instability limit its applications.[14,15]

Recently, a few studies on the Ti doped $BiFeO_3$ have shown the enhanced multiferroic properties.[16,17] Palkar and Malik[18] have reported the conversion of ferroelectric $PbTiO_3$ into multiferroic by partially substituting Ti with Fe. It has been also reported that Ni substituted $PbTiO_3$ system also shows magnetoelectric behaviour at room temperature.[19] The lead (Pb) based multiferroic compounds are toxic and non-eco friendly, which restricts their use. Recently, $Bi_4Ti_3O_{12}$ (BIT) has gained much attention as a substitute of Pb based compounds.[20] Layer structured bismuth titanate (BIT) belonging to the Aurivillius family of compounds (general formula $[Bi_2O_2]^{2+}$ $[A_{n-1}B_n\ O_{3n+1}]^{2-}$ with $n = 3$) possesses high ferroelectric transition temperature and is easy to process.[21] Recently, Chen *et al*. have reported the existence of multiferroicity in Fe doped BIT, but the system suffered from high losses due to conduction.[22,23]

To search for new type single phase lead free multiferroic materials showing magnetoelectric effect at room temperature, we have synthesized $Bi_{4-x}Sm_xTi_{3-x}Ni_xO_{12\pm\delta}$ compound by partially substituting nickel (Ni) at the Ti-site and samarium (Sm) at the Bi-site in BIT. Transition element

[a)]Author to whom correspondence should be addressed. Electronic mail: jp_phy@yahoo.in. Tel. +91-9418179401. Fax: +91 1972 223834.

Ni is substituted to induce magnetism in the ferroelectric BIT and the rare earth Sm to control the losses in the system, which might be due to oxygen vacancy related defects in BIT. It is reported that Sm substitution improves the ferroelectric and magnetic properties of the layered structured compounds.[24,25]

According to our knowledge, no report has been yet so far published on co-substitution of Sm and Ni in the BIT. In the present work, we have comprehensively studied the structural, dielectric, electrical, ferroelectric, magnetic, and magnetoelectric properties of $Bi_{4-x}Sm_xTi_{3-x}Ni_xO_{12\pm\delta}$ ($x = 0$, 0.02, 0.05, and 0.07) ceramics at room temperature.

II. EXPERIMENTAL DETAILS

Polycrystalline single phase $Bi_{4-x}Sm_xTi_{3-x}Ni_xO_{12\pm\delta}$ ($0 \le x < 0.1$) samples were synthesized by conventional solid state reaction method. Stoichiometric amounts of Bi_2O_3, TiO_2, Sm_2O_3, and NiO with purity >99.95% (Sigma Aldrich) were used as the starting material. For better homogeneity, the weighed powder of each composition with 3 wt. % excess Bi_2O_3 was ball milled in a Fritsch Pulverisette Planetary high energy ball milling system at room temperature. The milling speed was set 200 rpm. The milling was stopped for 20 min after every 60 min of milling to cool down the system. All compositions were milled for 5 h in tungsten carbide jars. The milled powder was calcined at 700 °C for 12 h. The calcined powder of each composition was then pressed into pellets of diameter 12 mm and thickness of 1–2 mm using hydraulic press at a pressure of 120 MPa. The final sintering of the pellets was done at 1000 °C for 4 h.

To study the crystallographic structures, x-ray diffraction (XRD) pattern of the ceramic samples was recorded with X′Pert PRO PANalytical Diffractometer using Cu K_α radiation ($\lambda = 1.54$ A°) over a 2θ range between $20° \le 2\theta \le 60°$ at scanning rate of 3°/min. Local structural distortions within the samples were studied using Raman spectroscopy (Reinshaw invia Raman microscope) equipped with Argon laser ($\lambda = 514.5$ nm) operated at 20 mW. The microstructures and elemental composition were investigated by using field emission scanning electron microscope (FESEM) of FEI Quanta FEG-450 with energy dispersion x-ray spectroscope (EDX) attached (Bruker-Nano-X-flash detector 5030), respectively. The dielectric properties of the sintered samples were measured by a LCR meter (Wayne Kerr 6500 B). DC resistivity of the samples with different composition at room temperature was measured using Keithley 6221 system. The ferroelectric measurements at room temperature were carried out using an automatic P-E loop tracer. Magnetization measurements were performed using vibrating sample magnetometer (Lake Shore Model No 662) at room temperature. The magnetoelectric effect was performed using the laboratory assembled dynamic magnetoelectric coupling set up.

III. RESULTS AND DISCUSSION

A. Structural and morphological studies

X-ray diffraction patterns of $Bi_{4-x}Sm_xTi_{3-x}Ni_xO_{12\pm\delta}$ ($x = 0$, 0.02, 0.05, 0.07, and 0.1) ceramic samples at room temperature sintered at 1000 °C are shown in Fig. 1. For $x \le 0.07$, all the diffraction peaks correspond to the pure phase of $Bi_4Ti_3O_{12}$ having orthorhombic structure (JCPDS card No. 89-7500). It is clearly evident from the XRD analysis that there is no change in structural symmetry except the small change in lattice parameters with Sm and Ni substitution. For $x > 0.07$, an impurity peak at around $2\theta = 28.11°$ (indicated by * in Fig. 1) may attributed to the secondary phase in the system. The peak is identified as bismuth nickel oxide ($Bi_{7.47}Ni_{0.53}O_{11.73}$) matched with (JCPDS card No. 43-0209). Therefore, the solubility of the Ni in BIT is only up to $x = 0.07$ concentration. The lattice parameters and unit cell volume computed for each composition are listed in Table I, which clearly reveal that the lattice parameters and unit cell volume change upon substitution. The lattice constants *a*, *c* increase while *b* decreases, leading to slight increase in unit cell volume. The variation in these parameters may be due to different ionic radii of Ni^{2+} (0.69Å) and Sm^{3+} (0.96Å) as compared to Ti^{4+} (0.61Å) and Bi^{3+} (1.03Å), respectively.[26] Such variations in the lattice parameter have increased the orthorhombic distortion defined as $\delta = 2(a-b)/(a+b)$.[27] The values of the δ are 5.53×10^{-4}, 1.66×10^{-3}, 2.58×10^{-3}, and 3.32×10^{-2} for $x = 0$, 0.02,

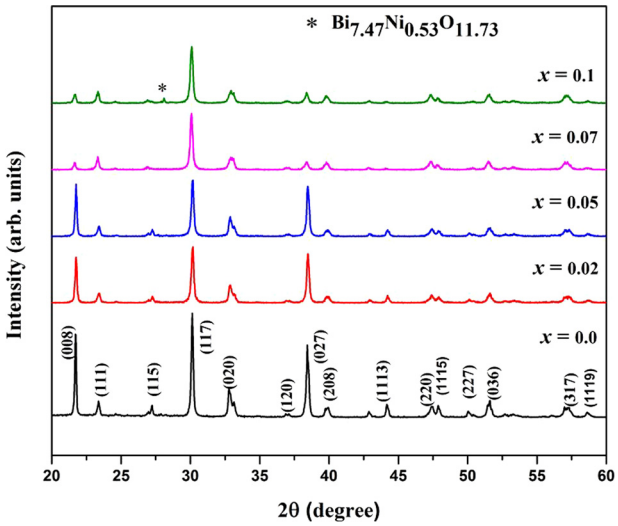

FIG. 1. XRD patterns of $Bi_{4-x}Sm_xTi_{3-x}Ni_xO_{12\pm\delta}$ ceramic with $x = 0$, 0.02, 0.05, 0.07, and 0.1.

TABLE I. Structural, electrical, dielectric, ferroelectric, magnetic, and magneto electric parameters of $Bi_{4-x}Sm_xTi_{3-x}Ni_xO_{12\pm\delta}$ ($x = 0.0$, 0.02, 0.05, and 0.07).

Parameters	$x = 0$	$x = 0.02$	$x = 0.05$	$x = 0.07$
Lattice parameters (Å)	a = 5.421	a = 5.423	a = 5.425	a = 5.428
	b = 5.418	b = 5.414	b = 5.411	b = 5.410
	c = 32.725	c = 32.740	c = 32.766	c = 32.810
Unit cell volume ($Å^3$)	961.16	961.25	961.88	963.48
Distortion (c/a)	6.036	6.037	6.039	6.044
ρ (Ω cm) at RT	2.2×10^7	1.46×10^8	2.69×10^8	3.86×10^8
T_c (°C)	674	690	716	722
2 P_r ($\mu C/cm^2$)	8.66	10.68	13.06	15.42
$2M_r$ (10^{-4} emu/g)	Diamagnetic	8.34	12.52	20.56
α_{max}(mV/cm Oe)	…	0.35	0.46	0.60

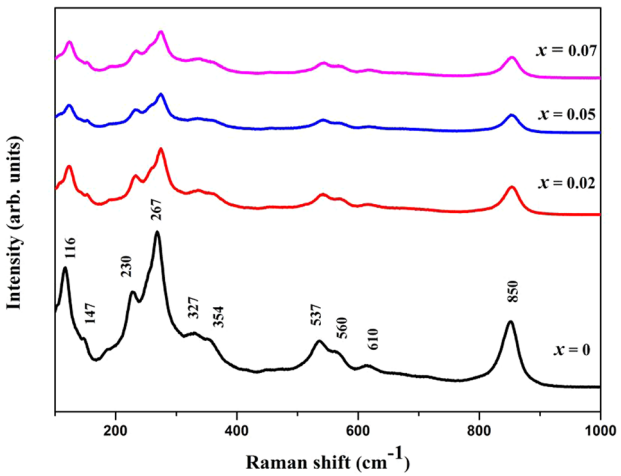

FIG. 2. Raman spectra of $Bi_{4-x}Sm_xTi_{3-x}Ni_xO_{12\pm\delta}$ ($x = 0$, 0.02, 0.05, and 0.07) at room temperature.

0.05, and 0.07 compositions, respectively. The distortion ratio (c/a) computed for each composition is also found to increase with substitution (listed in Table I). From the observed values of the distortion, it can be concluded that Sm and Ni substitution has increased the structural distortions in the system.

In order to understand the effect of substitution, Raman scattering study has proved to be very useful technique to provide information about local structures in the materials. Fig. 2 shows the Raman scattering spectra of $Bi_{4-x}Sm_xTi_{3-x}Ni_xO_{12\pm\delta}$ ($x = 0$, 0.02, 0.05, and 0.07) at room temperature. Theoretically, there are 24 Raman active modes for orthorhombic BIT.[28,29] However, as shown in Fig. 2, only the Raman modes at about 116, 147, 230, 267, 327, 354, 537, 560, 610, and 850 cm^{-1} were observed in pure BIT. The internal modes, which originate from TiO_6 octahedra, appear above 200 cm^{-1}.[28] The main modes at ~267 and 850 cm^{-1} have similar doping dependences; the peak broadening and reduction in the intensity with substitution indicating structural distortion in the environment of TiO_6 octahedra, due to the charge imbalance at the Ti-site. The modes at ~537 and 560 cm^{-1} and other two modes at ~327 and 354 cm^{-1} tend to merge with each other upon substitution, which corresponds to the distortion in the TiO_6 octahedra caused by A-site substitution in terms of change in the strength of Bi-O bond.[30,31] The Raman mode at ~116 cm^{-1} is due to the vibration of Bi at the A-site. The small shift of this mode towards higher vibrational frequency is due to the substitution of lighter Sm atom at the Bi-site with gradual decrease in its intensity with decreasing Bi content.[32] The structural distortions observed in XRD pattern were also observed at the local level in the Raman spectra. Hence, the results obtained from the Raman spectra correlate well with the XRD pattern.

The FE-SEM micrographs of $Bi_{4-x}Sm_xTi_{3-x}Ni_xO_{12\pm\delta}$ for $x = 0$, 0.02, 0.05, and 0.07 are shown in Fig. 3. The morphology of each sample clearly shows the formation of randomly oriented plate like grains. It can be noticed from Fig. 3 that the grain size increases gradually with the substitution of Sm and Ni, which might be due to the expansion of the unit cell along a and c-axis, and improved sintering conditions. There is no additional phase segregation has been observed in the system. The elemental composition analysis of each sample by EDX as shown in Fig. 4 confirms that Sm and Ni are well incorporated into the system. The weight and

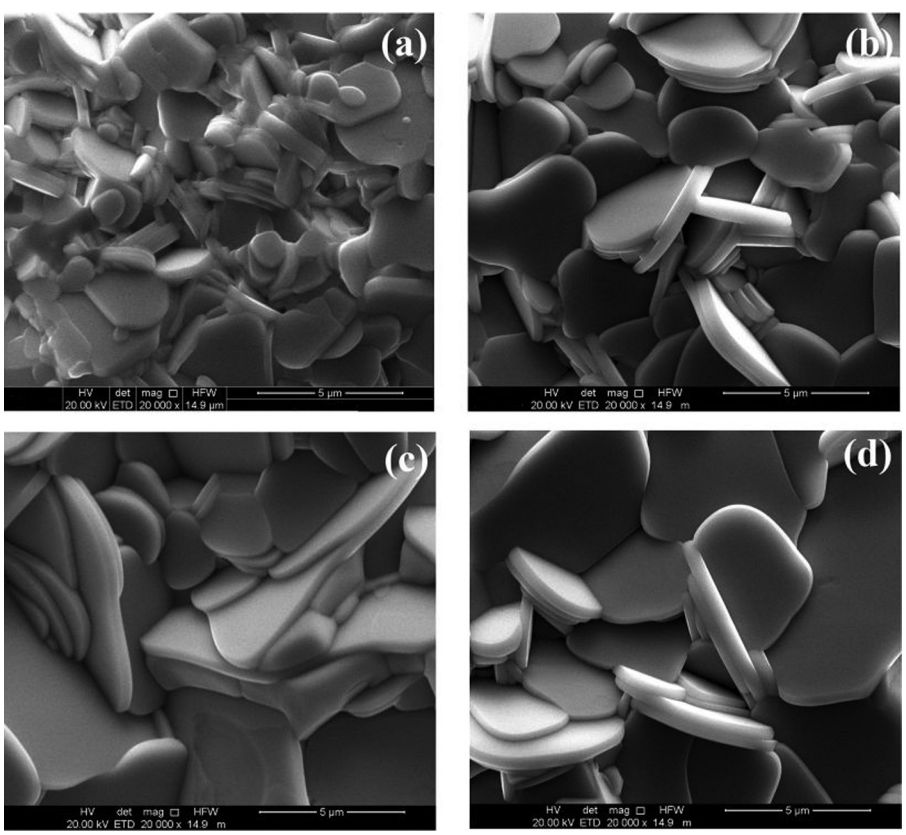

FIG. 3. FE-SEM surface micrographs of $Bi_{4-x}Sm_xTi_{3-x}Ni_xO_{12\pm\delta}$ for (a) $x = 0$, (b) $x = 0.02$, (c) $x = 0.05$, and (d) $x = 0.07$.

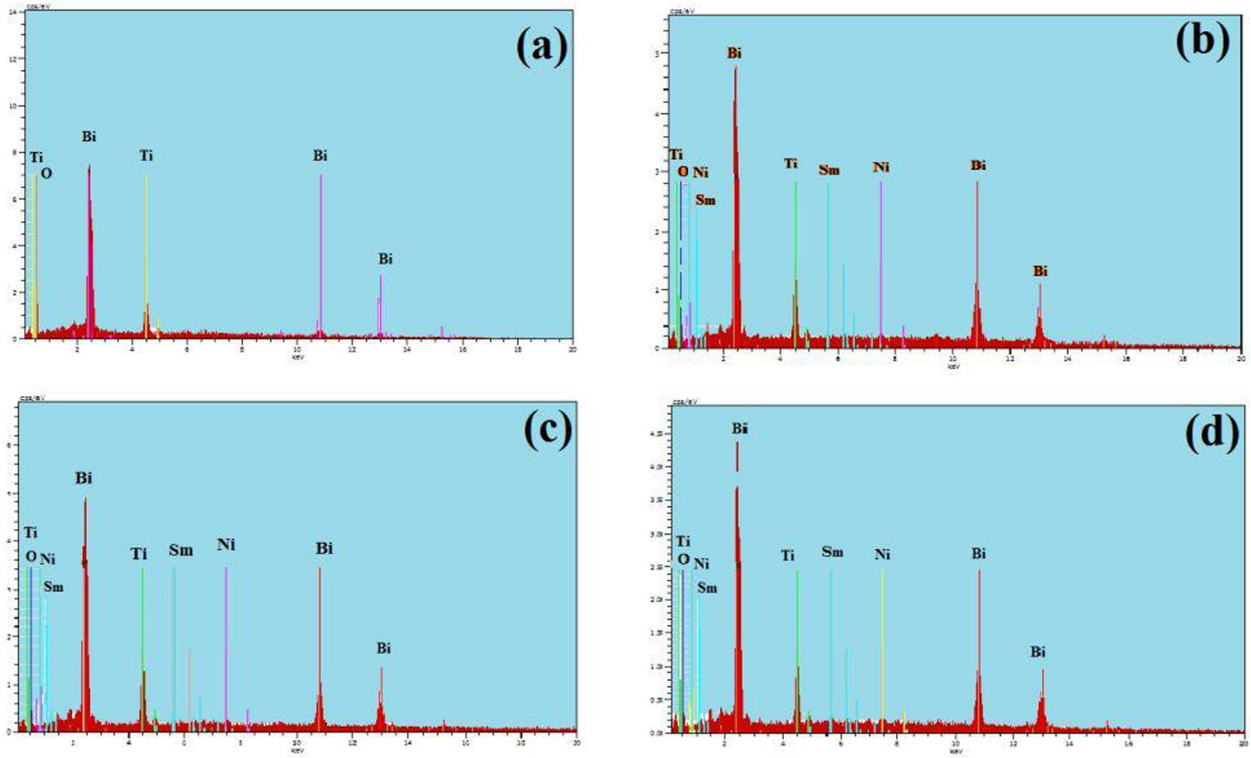

FIG. 4. EDX of $Bi_{4-x}Sm_xTi_{3-x}Ni_xO_{12\pm\delta}$ ceramics for (a) $x=0$, (b) $x=0.02$, (c) $x=0.05$, and (d) $x=0.07$.

atomic percentage observed in each sample are given in Table II.

B. Dielectric studies

Figure 5(a) shows the variation of dielectric constant (ε') at room temperature as a function of frequency over the range of 1 kHz–1 MHz for all the ceramic samples $Bi_{4-x}Sm_xTi_{3-x}Ni_xO_{12\pm\delta}$ ($0 \le x \le 0.07$). The dielectric constant has been found to decrease with increasing content of Sm and Ni in the specimen. The dielectric constant exhibits a strong dispersion in low frequency region (<10 kHz) for x = 0. The observed decrease in dielectric constant with increase in Sm and Ni content at all frequencies may be attributed to a possible reduction in the space charge effect. The dependence of dielectric constant on the frequency is due to the space charge polarization. During heat treatment, the volatile nature of Bi might create defects in the system due to oxygen vacancies. These defects along with $6s^2$ lone pair of Bi contribute to the space charge polarization. The decrease in dispersion of the dielectric constant upon substitution indicates the reduced charge effects, due to the reduction of oxygen vacancies and number of $6s^2$ lone pairs. In the samples substituted with Sm and Ni, there is almost negligible dispersion in dielectric constant beyond 10 kHz as against 100 kHz for pure BIT. Hence, Sm plays the major role to reduce the defects in the system. We can draw the similar inference from the frequency dependence loss tangent (tan δ) curves for these specimens as shown in Fig. 5(b), where the pure sample appears to be more conducting as compared to the samples with Sm and Ni content. The loss tangent curve represents the absorption of energy or dielectric loss due to the lagging of orientation polarization behind the applied field. Moreover, the room temperature (RT) dc resistivity (ρ) of the ceramics increases upon substitution as shown in Table I. All these results exhibit the improved dielectric properties of BIT when co-substituted with Sm and Ni.

TABLE II. EDX analysis of $Bi_{4-x}Sm_xTi_{3-x}Ni_xO_{12\pm\delta}$ ($x=0.0$, 0.02, 0.05, and 0.07).

	$x=0$		$x=0.02$		$x=0.05$		$x=0.07$	
Elements	Wt. %	At %	Wt. %	At. %	Wt. %	At. %	Wt. %	At. %
Bi L	74.13	23.76	74.05	23.62	74.11	23.80	73.73	23.52
Ti K	11.51	16.10	11.29	15.71	10.98	15.40	11.03	15.37
O K	14.36	60.14	14.31	59.65	14.40	60.47	14.56	60.43
Sm L	…	…	0.15	0.07	0.34	0.15	0.45	0.20
Ni K	…	…0.08	0.09		0.15	0.18	0.21	0.24

The measurement of dielectric constant (ε') as a function of temperature carried out at 100 kHz for all the ceramic samples is shown in Fig. 6(a). Dielectric measurement shows peaks around 674, 690, 716, and 722 °C, which correspond to the ferroelectric phase transition for $x=0$, 0.02, 0.05, and 0.07 samples, respectively. It is clearly observed that the ferroelectric transition temperature (T_c) increases with increasing content of Sm and Ni, as a consequence of increased orthorhombic distortions in the system.[33] Decrease in dielectric constant upon increasing substitution may be attributed to the decrease in the interfacial or space charge polarization. The decrease in the interfacial polarization is also supported by the results obtained from the FE-SEM (Fig. 3), which reveals that the size of the grain increases with increasing

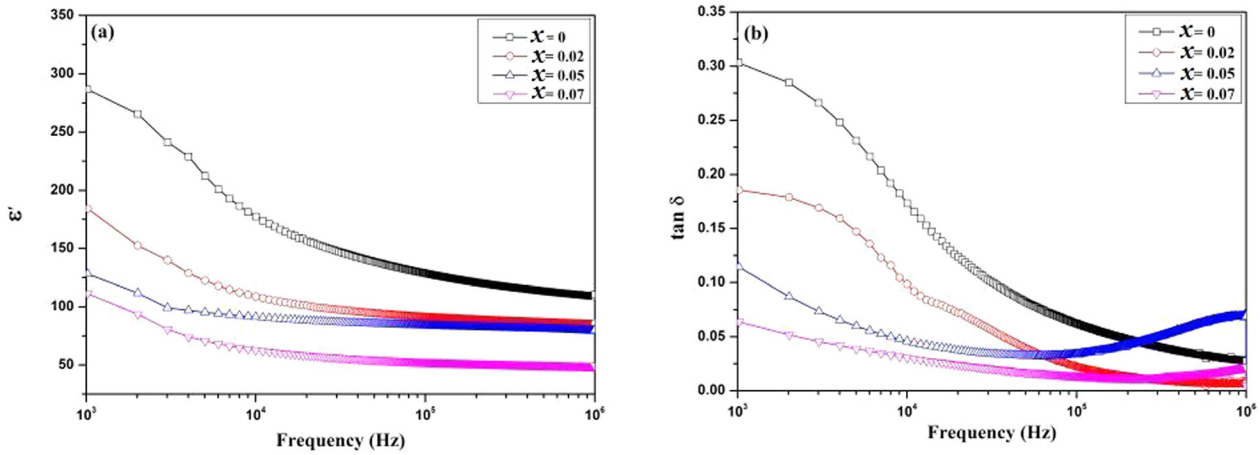

FIG. 5. Frequency dependence of (a) dielectric constant (ε'), (b) loss tangent ($\tan\delta$) of $Bi_{4-x}Sm_xTi_{3-x}Ni_xO_{12\pm\delta}$ ($x = 0$, 0.02, 0.05, and 0.07) at room temperature.

content of Sm and Ni in BIT. The growth in the grain size reduces the volume fraction of grain boundaries, resulting decrease in the interfacial polarization. Similar inferences can be drawn from the temperature dependent loss tangent curves as shown in Fig. 6(b).

C. Ferroelectric studies

Figure 7 shows the ferroelectric hysteresis loops at room temperature for all the considered samples measured at a fixed ac frequency of 50 Hz under the maximum applied electric field (30 kV/cm). It can be observed from the loops that all the samples exhibit ferroelectric behaviour. The measured values of remnant polarization ($2P_r$) are 8.66, 10.68, 13.06, and 15.42 $\mu C/cm^2$ for $x = 0$, 0.02, 0.05, and 0.07 samples, respectively (also shown in Table I). Such type of behaviour for the samples $x = 0$ and $x = 0.02$ may be due to the trapped defect states and not to demonstrate the true ferroelectric behaviour.[34,35] To overcome this problem, we have measured the P-E loops at various frequencies (see inset of Figs. 7(a) and 7(b)). From the frequency dependent P-E loops, we have observed that there is a marginal variation in the shape of the hysteresis loops and the value of P_r and E_c for $x = 0$ and $x = 0.02$, whereas there is no such variation observed for $x = 0.05$ and $x = 0.07$ samples, respectively. The improvement in the shape of the ferroelectric loops with substitution indicates the decrease in the conductivity of the samples, due to the decreasing defects in the system. The increased $2P_r$ is a consequence of increasing distortion in the system upon substitution.[36] The increase in $2P_r$ might be due to the enhancement of grain size. The gradual increase in grain size, which can be easily observed from the FE-SEM micrograph, decreases the volume fraction of grain boundaries. This decreases the space charge probability trapped at the boundary and reduces the pinning of the neighbouring domains. Also the increase in grain size weakens the segregation of the defects at the domain walls. The reduction in both pinning effect as well as segregation of defects helps to speed up the movement of the domain walls, which results an increase in the remnant polarization.[37] Hence, the combined effect of distortion and grain size has improved the ferroelectric properties of the $Bi_{4-x}Sm_xTi_{3-x}Ni_xO_{12\pm\delta}$ system.

D. Magnetization studies

Figure 8 shows the isothermal magnetization hysteresis loops for $Bi_{4-x}Sm_xTi_{3-x}Ni_xO_{12\pm\delta}$ at room temperature. An anti S-type magnetization-field (M-H) curve has been

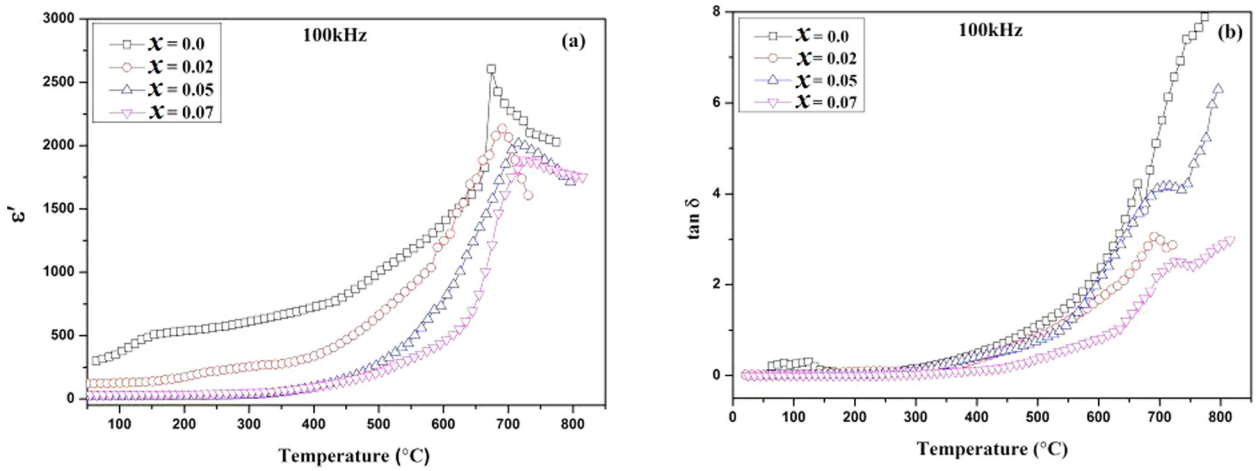

FIG. 6. Temperature dependence of (a) dielectric constant (ε'), (b) loss tangent ($\tan\delta$) of $Bi_{4-x}Sm_xTi_{3-x}Ni_xO_{12\pm\delta}$ ($x = 0$, 0.02, 0.05, and 0.07) at 100 kHz.

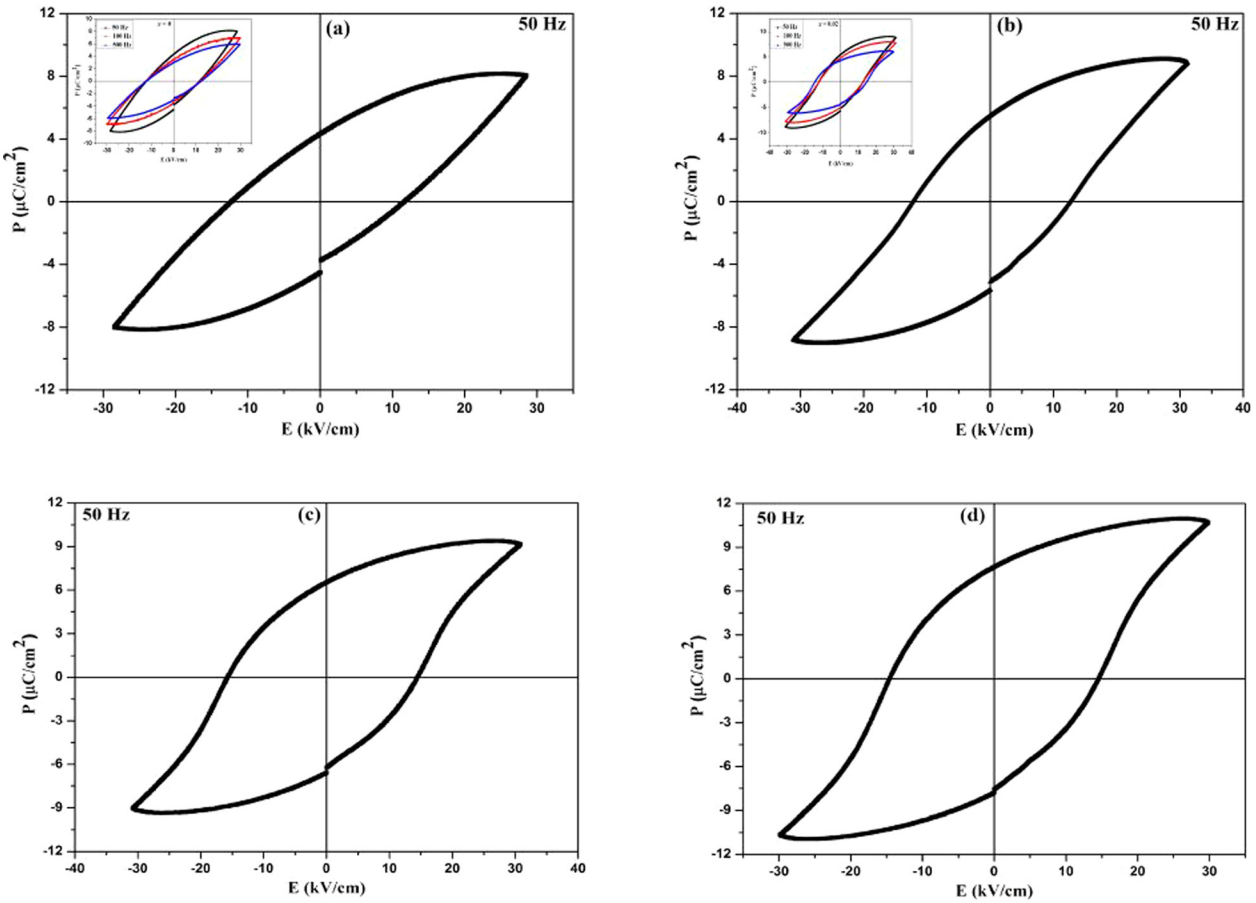

FIG. 7. P-E hysteresis loops of the $Bi_{4-x}Sm_xTi_{3-x}Ni_xO_{12\pm\delta}$ ceramics for (a) $x=0$, (b) $x=0.02$, (c) $x=0.05$, and (d) $x=0.07$ at room temperature.

obtained for pure ($x=0$) sample, demonstrating the diamagnetic nature of $Bi_4Ti_3O_{12}$. The M-H curve changes gradually into S-type hysteresis loop with increasing content of Sm and Ni, indicating that magnetism in the system starts arising due to the incorporation of magnetic ions. It can be observed that a loop is formed at the lower field and a non-saturated behaviour occurs at the higher field. The non-saturation of the hysteresis loop indicates that the system is magnetically disordered, i.e., spins are canted instead of being parallel or anti-parallel. The remnant magnetization ($2M_r$) for $x=0.02$, 0.05, and 0.07 is 8.34×10^{-4}, 12.52×10^{-4}, and 20.56×10^{-4} emu/g, respectively. The enhanced magnetism might be explained by the following factors.

When the magnetic Ni^{2+} ions are substituted at the B-site, different types of magnetic network exist in the system, leading to different types of interactions between these ions. One type of network that may exist is the Ni^{2+}-□-Ni^{2+}, where (-□- denotes oxygen vacancy). The electron trapped in the oxygen vacancy will form the F-centre.[38] The F-centre is similar to bound magnetic polaron.[39] The magnetic interaction between Ni^{2+} ions via F-centre gives rise to ferromagnetic (FM) order. In another network, such as Ni^{2+}-O-Ni^{2+}, the super-exchange interaction between the magnetic ions will favour the anti-ferromagnetic (AFM) order. The competing FM and AFM orders lead to magnetic disorder, which result canted spins. Further, due to the perovskite layered structure of bismuth titanate, the spins of Sm^{3+} ions in the sub-lattices are canted. This leads to weak canted antiferromagnetic behaviour.[25] The extent of canting of spin structure increases with the substitution of Sm^{3+} ions. Hence, the co-substitution of Sm and Ni has enhanced the magnetic properties of the system.

E. Magnetoelectric studies

The ferroelectric and magnetization studies reveal that both ferroic orders exist in $Bi_{4-x}Sm_xTi_{3-x}Ni_xO_{12\pm\delta}$ ceramic for $x=0.02$, 0.05, and 0.07, respectively. To observe the mutual dependence of these orders in a single phase material, the ME effect which is characterized by the magneto-electric coupling co-efficient ($\alpha=dE/dH$) is measured in terms of induced electric field under applied ac magnetic field.[40] The dc bias magnetic field (H_{dc}) up to 6 kOe is produced by an electromagnet and an ac magnetic field ($H_{ac}=3$ Oe) produced by a pair of Helmholtz coils were superimposed in a sample. The ME voltage across each sample under applied dc magnetic field at a constant ac magnetic field was measured by lock-in-amplifier. Fig. 9 shows the variation of α as a function of applied dc magnetic field (H_{dc}) at a fixed ac magnetic frequency (993 Hz) for $Bi_{4-x}Sm_xTi_{3-x}Ni_xO_{12\pm\delta}$ ($x=0.02$, 0.05, and 0.07), measured at room temperature. The coupling co-efficient shows a non-linear behaviour with applied dc magnetic bias for all the samples. The optimized H_{dc} at which α is a maximum, shift towards higher field. The maximum values of coupling co-efficient are 0.35, 0.46, and 0.60 mV/cm Oe for $x=0.02$, 0.05, and 0.07, respectively,

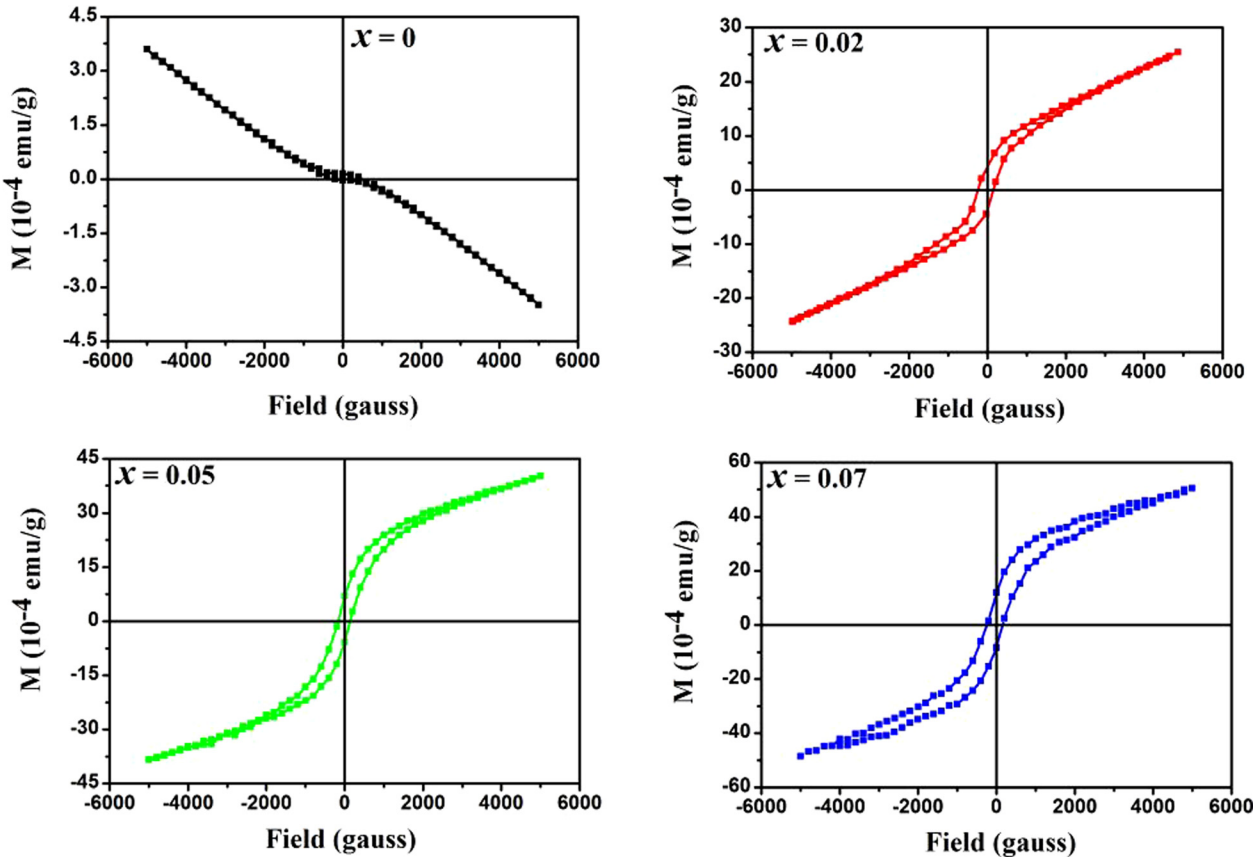

FIG. 8. M-H hysteresis loops for the $Bi_{4-x}Sm_xTi_{3-x}Ni_xO_{12\pm\delta}$ ($x = 0$, 0.02, 0.05, and 0.07) ceramics at room temperature.

which increase with the increase in substitution content (also see Table I). In single phase multiferroic materials, the ME coupling arises mainly from the interaction between electric and magnetic sub-lattices through the stress or strain transmitting from one sub-lattice to another.[41] The observed value of ME coupling coefficient is low and is comparable with the reported value on composite materials, which are established as multiferroics.[40,42]

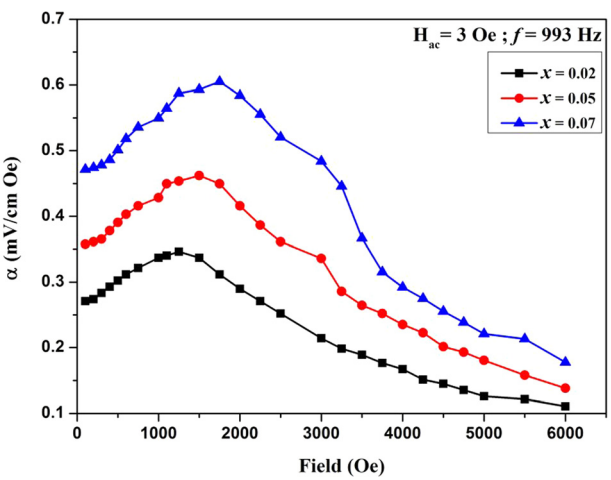

FIG. 9. Variation of magneto-electric coupling co-efficient (α) with dc bias field (H_{dc}) at magnetic frequency f = 993 Hz for $Bi_{4-x}Sm_xTi_{3-x}Ni_xO_{12\pm\delta}$ ceramics with $x = 0.02$, 0.05, and 0.07.

IV. CONCLUSIONS

Multiferroic $Bi_{4-x}Sm_xTi_{3-x}Ni_xO_{12\pm\delta}$ ceramic with $x = 0.02$, 0.05, and 0.07 has been synthesized by conventional solid state reaction technique. Partial substitutions by Sm^{3+} and Ni^{2+}ions have increased the orthorhombic distortion, distortion ratio c/a, grain size, and ferroelectric transition temperature. The decrease in dielectric loss and the increase in dc resistivity at room temperature signify the reduction in the conduction, which results in relatively low leakage. Both good ferroelectric and magnetic properties are exhibited by the present ceramics at room temperature. The magneto-electric coupling between the electric and magnetic dipoles is demonstrated by measuring the ME output voltage as a result of applied dc bias magnetic field. The magnetoelectric coupling co-efficient increases with increase in substitution content and observed a maximum value of 0.60 mV/cm/Oe. The results of ME coupling demonstrate the multiferroic behaviour of Sm and Ni substituted $Bi_{4-x}Sm_xTi_{3-x}Ni_xO_{12\pm\delta}$ system. Hence, these multiferroic materials may be useful for designing cost effective electromagnetic devices.

ACKNOWLEDGMENTS

The authors would like to acknowledge Dr. Nagesh Thakur, Dr. N. S. Negi, and Dr. Mahavir Singh, Department of Physics, Himachal Pradesh University, Shimla, India for providing facilities for dielectric, ferroelectric, and magnetic

measurements. Joginder Paul is thankful to the Department of Higher Education, Himachal Pradesh, India for proving study leave to conduct this work.

[1]H. Schmid, Ferroelectrics **162**, 317 (1994).
[2]M. Fiebig, J. Phys. D: Appl. Phys. **38**, R123 (2005).
[3]W. Erenstein, N. D. Mathur, and J. F. Scott, Nature **442**, 759 (2006).
[4]N. Hur, S. Park, P. A. Sharma, J. S. Ahn, S. Guha, and S. W. Cheong, Nature **429**, 392 (2004).
[5]H. Schmid, Ferroelectrics **252**, 41 (2001).
[6]S. V. Suryanarayana, Bull. Mater. Sci. **17**, 1259 (1994).
[7]N. A. Hill, J. Phys. Chem. B **104**, 6694 (2000).
[8]H. Zheng, J. Wang, S. E. Lofland, Z. Ma, L. M. Ardabili, T. Zhao, L. S. Riba, S. R. Shinde, S. B. Ogale, F. Bai, D. Viehland, Y. Jia, D. G. Schlom, M. Wuttig, A. Roytburd, and R. Ramesh, Science **303**, 661 (2004).
[9]F. Jona and G. Shirane, *Ferroelectric Crystals* (Dover, New York, 1993).
[10]D. I. Khomskii, Bull. Am. Phys. Soc. C **21**, 2 (2001).
[11]M. Fiebig, T. Lottermoser, D. Frohlich, A. V. Goltsev, and R. V. Pisarev, Nature **419**, 818 (2002).
[12]M. Muto, Y. Tanabe, T. I. Sakano, and E. Hanamura, Phys. Rev. B **57**, 9586 (1998).
[13]T. Kimura, T. Goto, H. Shinatani, K. Ishizaka, T. Arima, and Y. Tokura, Nature **426**, 55 (2003).
[14]Y. P. Wang, L. Zhou, M. F. Zhang, X. Y. Chen, J. M. Liu, and Z. G. Liu, Appl. Phys. Lett. **84**, 1731 (2004).
[15]J. R. Cheng, N. Li, and L. E. Cross, J. Appl. Phys. **94**, 5153 (2003).
[16]M. Kumar and K. L. Yadav, J. Appl. Phys. **100**, 074111 (2006).
[17]M. Kumar and K. L. Yadav, J. Phys.: Condens. Matter **18**, L503 (2006).
[18]V. R. Palkar and S. K. Malik, Solid State Commun. **134**, 783 (2005).
[19]M. Kumar and K. L. Yadav, J. Appl. Phys. **102**, 076107 (2007).
[20]J. M. Herbert, *Electrocomponent Science Monograph*, 3rd ed. (Gordon & Breach, New York, 1982).
[21]T. Jardiel, A. C. Caballero, and M. Villegas, J. Ceram. Soc. Jpn. **116**, 511 (2008).
[22]X. Q. Chen, F. J. Yang, W. Q. Cao, D. Y. Wang, and K. Chen, J. Phys. D: Appl. Phys. **43**, 065001 (2010).
[23]X. Q. Chen, F. J. Yang, W. Q. Cao, D. Y. Wang, and K. Chen, Solid State Commun. **150**, 1221 (2010).
[24]T. Shigyo, H. Kiyono, and J. Nakano, Jpn. Soc. Appl. Phys. **47**, 7617 (2008).
[25]A. Srinivas, F. Y. C. Boey, and T. Sritharan, Mater. Sci. Eng., B **123**, 222 (2005).
[26]R. D. Shannon, Acta Crystallograph., Sect. A **32**, 751 (1976).
[27]Y. Shimakawa, Y. Kubo, Y. Tauchi, H. Asano, T. Kamiyama, F. Izumi, and Z. Hiroi, Appl. Phys. Lett. **79**, 2791 (2001).
[28]S. Kojima and S. Shimada, Phys. B: Condens. Matter **219**, 617 (1996).
[29]S. Kojima, Ferroelectrics **239**, 55 (2000).
[30]P. R. Graves, G. Hua, S. Myhra, and J. G. Thompson, J. Solid State Chem. **114**, 112 (1995).
[31]A. Hushur, J. H. Ko, S. Kojima, S. S. Lee, and M. S. Jang, J. Korean Phys. Soc. **41**, 763 (2002).
[32]D. Wu, A. D. Li, T. Zhu, Z. F. Li, Z. G. Liu, and N. B. Ming, J. Mater. Res. **16**, 1325 (2001).
[33]S. Rachna, S. Bhattacharyya, and S. M. Gupta, Mater. Sci. Eng., B **175**, 207 (2010).
[34]L. Pintilie and M. Alexe, Appl. Phys. Lett. **87**, 112903 (2005).
[35]J. F. Scott, J. Phys. Condens. Mater. **20**, 021001 (2008).
[36]A. Garg, Z. H. Barber, M. Dawber, J. F. Scott, A. Snedden, and P. Light, Appl. Phys. Lett. **83**, 2414 (2003).
[37]Q. Y. Jiang, E. C. Subbarao, and L. E. Cross, J. Appl. Phys. **75**, 7433 (1994).
[38]J. M. D. Coey, A. P. Douvalis, C. B. Fitzgerald, and M. Venkatesan, Appl. Phys. Lett. **84**, 1332 (2004).
[39]T. Kasuya, Solid State Commun. **8**, 1635 (1970).
[40]A. Singh, A. Gupta, and R. Chatterjee, Appl. Phys. Lett. **93**, 022902 (2008).
[41]A. Srinivas, D. W. Kim, K. S. Hong, and S. V. Suryanarayan, Appl. Phys. Lett. **83**, 2217 (2003).
[42]C. W. Nan, M. I. Bichurin, S. Dong, D. Viehland, and G. Srinivasan, J. Appl. Phys. **103**, 031101 (2008).